Cement and Concrete Composites 129 (2022) 104506

Contents lists available at ScienceDirect

Cement and Concrete Composites

journal homepage: www.elsevier.com/locate/cemconcomp

Shrinkage prediction of recycled aggregate structural concrete with alternative binders through partial correction coefficients

Víctor Revilla-Cuesta [a,e,*], Luís Evangelista [b,e], Jorge de Brito [c,e], Marta Skaf [d], Juan M. Manso [a]

[a] Department of Civil Engineering, Escuela Politécnica Superior, University of Burgos, c/ Villadiego s/n, 09001, Burgos, Spain
[b] Department of Civil Engineering, Instituto Superior de Engenharia de Lisboa - IPL, R. Conselheiro Emídio Navarro 1, 1959-007, Lisbon, Portugal
[c] Department of Civil Engineering, Architecture and Georresources, Instituto Superior Técnico, University of Lisbon, Av. Rovisco Pais 1, 1049-001, Lisbon, Portugal
[d] Department of Construction, Escuela Politécnica Superior, University of Burgos, c/ Villadiego s/n, 09001, Burgos, Spain
[e] CERIS-ICIST, Instituto Superior Técnico, University of Lisbon, Av. Rovisco Pais 1, 1049-001, Lisbon, Portugal

ARTICLE INFO

Keywords:
Recycled aggregate structural concrete
Reactive magnesium oxide
Ground granulated blast furnace slag
Shrinkage-prediction model
Partial correction coefficient
Prediction interaction

ABSTRACT

Estimating the shrinkage of structural concrete is essential to calculate, at the design stage, the stresses that a structure may experience due to this phenomenon. Nevertheless, changes in composition, as well as the use of wastes as raw materials, alter the shrinkage behaviour of concrete and render invalid shrinkage-prediction models from the standards. This paper shows a procedure to estimate the shrinkage of recycled aggregate concrete made with alternative binders. This procedure is based on modifying the shrinkage estimated through the Eurocode 2 or ACI 209.2R models by multiplying it by a partial correction coefficient for every change in concrete composition. The application of this procedure to high-performance and self-compacting concretes made with various contents of recycled aggregate of different maturity, reactive magnesium oxide and ground granulated blast furnace slag showed that it is suitable for estimating long-term shrinkage with maximum deviations of ±10%. However, to obtain an adequate accuracy, it is necessary to bear in mind some tips, such as the need to consider the prediction interactions between the factors, the usefulness of the natural logarithm of the concrete age to improve the estimation accuracy or the convenience of introducing a concrete-age-dependent coefficient to reach accurate shrinkage estimations at early ages. Finally, the partial correction coefficients are found to be of a simpler nature for the ACI 209.2R model, so this model is recommended for predicting the shrinkage of recycled aggregate concrete.

1. Introduction

Apparently, any structural concrete element has constant dimensions over time. However, those elements undergo notable dimensional variations during all its service life, which are mainly due to two aspects. On the one hand, the temperature variations to which they are exposed. Thermal oscillations between day and night or between the different seasons of the year cause concrete to expand (positive temperature increase) or contract (negative temperature increase) [1]. On the other hand, concrete always experiences shrinkage [2,3]. This phenomenon can be defined as the contraction of the cementitious matrix of concrete due to the delayed loss of water [4], either by deferred hydration of the cement (autogenous shrinkage) or by water evaporation (drying shrinkage) [5]. Although shrinkage occurs throughout the entire life of concrete, it is more pronounced at early ages due to the tensile capillary pressure that water evaporation causes after mixing (plastic shrinkage) [6]. Plastic shrinkage, in turn, often leads to concrete cracking, and shrinkage compensation design is therefore sometimes necessary to reduce it [7].

Dimensional variations play a key role on the failure design of concrete structures, as they cause the appearance of important stresses, especially in hyperstatic structures, which need to be accurately evaluated [8,9]. The magnitude of these stresses will be estimated according to the design values of the thermal and shrinkage strains [2,3]. Thus, the thermal strain is usually estimated assuming that it is directly proportional to the temperature [1], the constant of proportionality being the linear thermal expansion coefficient [10]. The estimation of shrinkage strain is not so simple since the shrinkage behaviour of concrete is closely linked to its composition [11]. The different US and European standards include a relatively easy specific formulation for the calculation of these magnitudes [2,12], but with the limitation that the concrete

* Corresponding author. Department of Civil Engineering, Escuela Politécnica Superior, University of Burgos, Calle Villadiego s/n, 09001, Burgos, Spain.
E-mail address: vrevilla@ubu.es (V. Revilla-Cuesta).

https://doi.org/10.1016/j.cemconcomp.2022.104506
Received 26 January 2022; Received in revised form 11 March 2022; Accepted 23 March 2022
Available online 25 March 2022

Acronyms

GGBFS	ground granulated blast furnace slag
HPC	high-performance concrete
MgO	magnesium oxide
NA	natural aggregate
OPC	ordinary Portland cement
RA	recycled aggregate
SCC	self-compacting concrete

considered in the development of those models was vibrated and made with conventional materials such as ordinary Portland cement (OPC) and natural aggregate (NA) [13,14].

In recent years, high-performance concrete (HPC) or self-compacting concrete (SCC) are increasingly common due to the advantages of their use [15,16]. However, their shrinkage performance is very different from that of conventional vibrated concrete. On the one hand, HPC is characterized by a higher cement content than usual, which results in very high strength [17], but at the same time increases the hydration heat [18], which in turn leads to higher shrinkage [19,20]. On the other hand, SCC is a type of concrete that requires no vibration during placement due to its high flowability, which means that it can be effectively adapted to formworks of any shape [21]. However, its high proportion of fine aggregate, necessary to obtain such high flowability, also means that in this type of concrete there are less coarse aggregate particles that oppose the cementitious-matrix contraction [22], which results in increased shrinkage levels [23].

The search for greater sustainability in construction materials is leading to the fact that different wastes or industrial by-products are being revalued as raw materials for the production of concrete, either as aggregate or as binder [24,25]. These sustainable raw materials are even being used in the manufacture of HPC and SCC [16,18], whose shrinkage patterns are modified when adding those raw materials [26,27]. Among the raw materials that can be considered, there are three that, according to existing studies, have a notable effect on concrete shrinkage:

- Recycled aggregate (RA) normally consists of sized crushed concrete, eventually from precast concrete elements [28]. The larger particles of this aggregate are NA with adhered cementitious matrix, while unhydrated cement and mortar can be found in the finest fractions [29], which allow RA powder to be used as a partial replacement for OPC [30]. Generally, these aspects cause the strength of concrete to decrease when RA is added, although correct mix design allows reaching strengths higher than 50 MPa [31]. On the other hand, RA composition also causes it to have greater flexibility than NA, so RA exhibits a lower opposition when the cementitious matrix contracts [11]. Furthermore, RA has a higher water absorption than NA, which makes this alternative aggregate absorb a greater amount of water during the mixing process of concrete [32] and, therefore, release a higher amount of water in a deferred way that later evaporates [33]. Both phenomena increase concrete shrinkage [11]. Conversely, RA's higher water absorption reduces autogenous shrinkage, *i.e.* shrinkage caused by delayed cement hydration [33], since its high water absorption levels allow replacing the water consumed in that process in a more efficient way [34];
- Ground granulated blast furnace slag (GGBFS) is a slag type produced by grinding blast furnace slag [35]. It is characterized by its binder characteristics, as well as its lower strength and stiffness than OPC's [36], so its use leads to concrete with worse mechanical behaviour [37]. However, despite its lower stiffness, its use reduces concrete shrinkage [38]. This trend is explained by its high grinding fineness [39], which helps to create a compact microstructure that hinders water evaporation from concrete [40], in addition to guaranteeing higher water availability for delayed cement hydration [41];
- Magnesium oxide (MgO) is a commercial product that can be used as an alternative binder. It is mainly characterized by its expansive properties, because when it reacts with water it turns into magnesium hydroxide, a chemical compound with a larger volume than MgO [42]. This expansion allows reducing concrete shrinkage [43]. However, it is essential to ensure that this expansion occurs at early ages, when the cementitious matrix has not yet developed its full stiffness. In other words, reactive MgO should be used [44]. In this way, concrete does not undergo a very pronounced micro-cracking due to MgO expansion, which could drastically worsen its mechanical behaviour [45]. Thus, an adequate balance between shrinkage reduction and mechanical-behaviour worsening is obtained [46]. Furthermore, the use of MgO also reduces the carbon footprint of concrete because its CO_2 emissions during manufacture are half compared to those of OPC [42].

The use of any of these alternative raw materials changes the shrinkage-prediction patterns of concrete [47]. Nevertheless, there are few models in the literature for predicting the shrinkage of recycled aggregate concrete [48,49], which are mainly based on understanding and modelling the RA factors that modify concrete shrinkage. Models for estimating the drying shrinkage of concrete when adding RA mainly depend on the amount of adhered mortar, the strength of the parent concrete, and the water absorption levels of RA [48]. On the other hand, the estimation of autogenous shrinkage requires the introduction of a factor that balances the lower stiffness and higher water absorption of RA compared to NA [49]. The available models that adopt a statistical approach are very scarce [11]. Furthermore, none of them address the prediction of the shrinkage of concrete simultaneously made with RA and alternative binders.

This study intends to show a simple procedure for the estimation of shrinkage of recycled aggregate concrete produced with any sustainable or alternative binder. This procedure, novel in the available literature, consists of modifying the models for shrinkage prediction of Eurocode 2 [2] and ACI 209.2R [12] with a partial correction coefficient for recycled aggregate and for every binder used in concrete production. These coefficients will depend on the amount of those materials, as well as on the prediction interactions that may exist between them. The proposed procedure is exemplified by obtaining the partial correction coefficients of 16 concrete mixes, both high-performance and self-compacting, manufactured with fine and coarse RA and two alternative binders, GGBFS and reactive MgO. It is shown that through this procedure the shrinkage estimation of any type of recycled aggregate structural concrete made with any binder is precise.

2. Materials and methods

2.1. Raw materials

2.1.1. Binder, water, and admixture

The 16 concrete mixes of this study were prepared using three binders:

- European standard ordinary Portland cement (OPC) as per EN 197–1 [50]. According to this standard, the OPC showed a density of about 3.1 Mg/m^3, a specific surface area of around 360 m^2/kg, and a content of ordinary clinker of 98%;
- CEM III/A 42.5 N European standard cement as per EN 197–1 [50]. This cement consisted of 55% OPC and 45% ground granulated blast furnace slag (GGBFS). According to the supplier, the density of this cement was 3.00 Mg/m^3, and its specific surface area 430 m^2/kg, lower than that of OPC;
- Reactive magnesium oxide (MgO). The MgO content in the chemical composition of the supplied product was 97%, while 95% of the

particles were less than 45 μm in size. Both aspects ensured optimum hydration and expansion of MgO when manufacturing the concrete [46]. The specific weight of reactive MgO was 3.58 Mg/m^3.

The concrete was produced with potable water obtained from the urban water supply network. A polycarboxylate-based superplasticiser admixture supplied by SIKA was used to provide an adequate level of workability for both high-performance and self-compacting mixes.

2.1.2. Aggregates

The concrete mixes developed in this research work analysed the effect of using recycled aggregate (RA) to replace natural aggregate (NA). Therefore, both NA and RA were used in the coarse and fine aggregate fractions, as described below:

- NA was crushed siliceous aggregate in the coarse fraction (4/22 mm), while it was rounded siliceous aggregate in the fine fraction (0/4 mm). The coarse fraction was used exclusively to produce HPC, while the fine fraction was used to produce both HPC and SCC, as shown and justified in the mix-design section;
- RA was produced by crushing a parent concrete with a compressive strength of 45 MPa on cubic specimens. After crushing, RA was sieved and separated into the fine fraction (0/4 mm) and two coarse fractions, 4/12.5 mm and 4/22 mm, respectively. The coarse fraction 4/12.5 mm was used to produce SCC, while the coarse fraction 4/22 mm was used in HPC, thus achieving adequate overall aggregate gradation in both concrete types [51,52]. In addition, the crushing of the parent concrete was performed at two different ages to analyse the effect of RA shrinkage on concrete shrinkage [34]. Therefore, both the coarse and fine RA fractions could be early-age RA, produced by crushing the parent concrete one week after casting, and matured RA, for which the parent concrete was crushed after six months curing.

Finally, SCC incorporated an aggregate powder in its composition, limestone fines 0/1 mm. The aim of this aggregate fraction was to provide the necessary fines content to reach a high level of self-compactability [53], as the fines content of the fine fraction of NA and RA was insufficient for this purpose.

The particle gradation of all aggregate fractions was continuous and suitable for concrete manufacturing (Fig. 1). On the other hand, the density and water absorption levels of all the aggregates exhibited usual values (Table 1) [54], the density of NA being higher than that of RA, and the water absorption of RA higher. All the aggregates were stored in the indoor environment of the laboratory during the research, with the coarse and fine RA presenting moisture contents of 0.6% and 0.9%, respectively. These moisture values, together with the production of trial mixes prior to the manufacture of the definitive mixes, enabled the water content and workability of concrete to be suitably adjusted.

Table 1
Water absorption and density of the aggregates as per EN 1097–6 [50].

Aggregate fraction	Water absorption at 24 h (%)	Density (Mg/m^3)
Coarse NA 4/22 mm	1.25	2.64
Coarse RA 4/22 mm [a]	4.89	2.43
Coarse RA 4/12.5 mm [a]	6.25	2.42
Fine NA 0/4 mm	0.72	2.60
Fine RA 0/4 mm [a]	7.07	2.38
Limestone fines 0/1 mm	2.53	2.61

[a] The water absorption levels in 24 h and the density were equal for early-age and matured RA.

2.2. Mix design

The mix design was carried out by fixing a constant workability degree for each concrete type. Therefore, the composition of concrete, especially the amount of water, was adjusted in each case, so that the addition of sustainable raw materials did not alter the workability. In this way, the results were not affected by the water content [11]. On the other hand, different ways of incorporating the sustainable raw materials were considered to evaluate the proposed shrinkage-estimation method in various situations. So, two ways for RA incorporation were performed: while in HPC the coarse and fine fractions of RA were simultaneously used to replace NA, in SCC the coarse fraction of NA was replaced first followed by the fine fraction.

2.2.1. HPC mixes

The design objective for the ten HPC mixes was to obtain in all cases a slump class S4, *i.e.* a slump between 160 mm and 210 mm (EN 206 [50]). The choice of such a high workability was justified by the fact that HPC should not only have high strength, but also optimum workability for placement in any location [34].

Firstly, the reference mix was designed, which was made with 100% OPC and NA. The proportions of OPC, coarse aggregate 4/22 mm, fine aggregate 0/4 mm, and water were set in accordance with Eurocode 2 [2]. Moreover, a superplasticiser (2% of cement mass) was added to

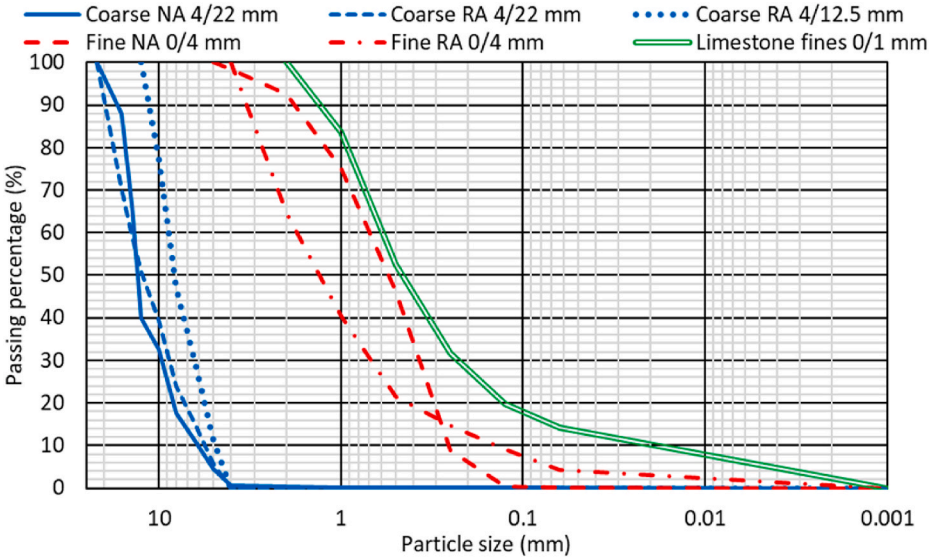

Fig. 1. Particle gradation of the aggregates (the particle gradation of early-age and matured RA was the same).

increase workability. These initial proportions were subsequently modified empirically to achieve the required workability.

Hereafter, the HPC mixes with OPC and RA (4 mixes) were designed. Their composition was the same as that of the reference concrete, but both coarse and fine RA replaced NA in proportions of 25% and 100% by volume. The incorporation of RA was carried out simultaneously in the coarse and fine aggregate fractions. Both matured (2 mixes) and early-age (2 mixes) RA was considered for this substitution.

Finally, the HPC mixes with MgO (5 mixes) were produced. For this purpose, reactive MgO replaced 10% OPC by mass in mixes with the same composition than the mixes with 100% OPC. This replacement ratio was chosen because literature studies have shown that it allows an adequate balance between the mechanical-behaviour loss and the shrinkage reduction that the expansion of MgO causes [45,46].

When using both reactive MgO and RA, the amount of water was adjusted due to the high water absorption levels of RA (Table 1), as well as the high specific surface area of MgO and, therefore, its higher water consumption for hydration than OPC [42]. This adjustment was made by considering the RA moisture and preparing trial mixes.

2.2.2. SCC mixes

For the six SCC mixes, a slump-flow class SF3 was sought, *i.e.* a slump flow from 750 mm to 850 mm (EN 206 [50]). The required workability class was set as high as possible to show the feasibility of achieving the highest SCC-flowability class with large amounts of alternative materials.

The reference mix was also first designed in SCC. It incorporated 100% OPC, 100% fine NA 0/4 mm, 100% coarse RA 4/12.5 mm, and limestone fines 0/1 mm. This initial coarse RA content was defined according to the findings of another study by the authors [55], which showed that there was no significant difference between the effect of adding 50% or 100% coarse RA on the mechanical behaviour of an SCC of this slump-flow class. So, it was also possible to evaluate the suitability of the proposed shrinkage-estimation procedure when using different ways for replacing NA with RA. The amounts of water and superplasticiser (2.2% cement mass) and the proportions of the different components were initially defined according to Eurocode 2 [2] indications and subsequently adjusted empirically.

SCC mixes with OPC and fine RA (2 mixes) were then produced. For that purpose, 50% and 100% fine NA was replaced with matured RA by volume correction. Again, these amounts of fine RA were defined according to the conclusions of the study mentioned above [55]. The water content was adjusted by means of RA moisture and trial mixes to keep the workability constant when adding fine RA.

Finally, the SCC mixes with 45% GGBFS (3 mixes) were produced using CEM III/A instead of OPC. The higher grinding fineness of GGBFS required the contents of coarse aggregate and cement to be adjusted, so that the SCC in the slump-flow test did not show any segregation and all aggregate particles were uniformly dragged.

2.2.3. Mix labelling

The concrete mixes were labelled with the code *"TC/FA-B"*, each term representing the following:

- *T*, concrete type: *HPC* or *SCC*;
- *C*, percentage of coarse RA: *0*, *25*, or *100*;
- *F*, percentage of fine RA: *0*, *25*, *50*, or *100*;
- *A*, RA's maturity: *blank* (no RA added), *E* (early-age RA), or *M* (matured RA);
- *B*, binder type: *blank* (100% OPC), *M* (90% OPC and 10% MgO), or *G* (55% OPC and 45% GGBFS).

Thus, for example, the mix HPC25/25E-M is an HPC made with 25% coarse and fine early-age RA and 10% reactive MgO. On the other hand, the mix SCC100/50M is an SCC made with 100% matured coarse RA, 50% matured fine RA and 100% OPC.

2.2.4. Composition and overall gradation

The composition of the mixes is shown in Table 2, while Fig. 2 depicts their overall size distributions. The replacement of NA with RA was nor conducted size by size, but simultaneously for all the sizes of the coarse (>4 mm) and fine (0/4 mm) aggregate fractions, as performed in other concrete-shrinkage studies [11]. This allowed maintaining the proportion between coarse and fine aggregate constant in all the mixes with respect to the reference mix, and did not significantly affect the overall gradation in the sizes corresponding to coarse aggregate. However, it did cause the overall size distribution in the fine fraction to have a higher proportion of larger-size particles as the content of fine RA increased. This aspect was not considered relevant, because the resistance of the aggregate to the contraction of the cementitious matrix produced by shrinkage is mainly due to the coarse aggregate [22], whose overall gradation was not modified. In addition, it was used to show that the proposed model allowed estimating shrinkage considering not only the effect of the lower stiffness and higher water absorption of RA, but also the effect of its particle gradation being different from that of NA.

2.3. Experimental tests

After concrete mixing, which was conducted in stages to maximise concrete workability [56], the fresh tests, slump test (EN 12350–2 [50]) for the HPC mixes and slump-flow test (EN 12350–8 [50]) for the SCC mixes, were performed. In this way, it was controlled that all the mixes exhibited the required workability. Subsequently, two 15 × 15 × 15-cm cubic specimens and two 10 × 10 × 50-cm prismatic specimens were produced for measuring compressive strength (EN 12390–3 [50]) and shrinkage (LNEC-E398 [57]), respectively:

- The cubic specimens were kept in a humid chamber (20 ± 2 °C and relative humidity 95 ± 5%) until 28 days, the standardised age at which compressive strength was measured [58];
- The prismatic specimens were stored in a dry room (20 ± 2 °C and relative humidity 40 ± 5%) from 1 to 91 days, period during which shrinkage was measured. The measurement times were defined according to the expected shrinkage levels, like in other similar studies [27,59]. Therefore, the length of the specimens was recorded more frequently at the beginning of the test (once a day) than at the end (once a week). Moreover, to obtain reliable shrinkage measurements, the length of every specimen at every age was measured 4 times, twice in each direction, using a digital comparator with a precision of ±1 μm.

2.4. Existing shrinkage-prediction models from standards

The partial correction coefficients for shrinkage estimation were obtained for the two most widespread existing models: the Eurocode 2 and the ACI 209.2R models. Both models are presented in this section.

2.4.1. European standard: Eurocode 2

In general, the autogenous shrinkage of concrete, caused by delayed hydration of cement, is very small compared to drying shrinkage, caused by water evaporation [47]. Therefore, it can be assumed that the total shrinkage of concrete, the sum of both types of shrinkage, is equal to the drying shrinkage for estimation purposes. This is reflected in the proposed model of the European standard (Eurocode 2 [2]), in which the estimated autogenous shrinkage is very small, practically negligible, compared to drying shrinkage.

Eurocode 2 estimates the drying shrinkage (ε_{cd}, mm/m) of concrete, and, therefore, the total shrinkage if the aspect indicated in the previous paragraph is considered as valid, through Equation (1).

Table 2
Mix design (kg/m^3).

Mix	OPC # MgO # CEM III/A	Limestone fines (0/1 mm)	Coarse NA # RA (4/22 mm)	Coarse NA # RA (4/12.5 mm)	Fine NA # RA (0/4 mm)	Water	Superplasticiser
HPC0/0	400 # 0 # 0	0	1080 # 0	0 # 0	850 # 0	150	8.0
HPC25/25M	400 # 0 # 0	0	815 # 245	0 # 0	640 # 190	160	8.0
HPC100/100M	400 # 0 # 0	0	0 # 980	0 # 0	0 # 760	195	8.0
HPC25/25E	400 # 0 # 0	0	815 # 245 [a]	0 # 0	640 # 190 [a]	160	8.0
HPC100/100E	400 # 0 # 0	0	0 # 980 [a]	0 # 0	0 # 760 [a]	195	8.0
HPC0/0-M	360 # 40 # 0	0	1080 # 0	0 # 0	850 # 0	165	8.0
HPC25/25M-M	360 # 40 # 0	0	815 # 245	0 # 0	640 # 190	175	8.0
HPC100/100M-M	360 # 40 # 0	0	0 # 980	0 # 0	0 # 760	210	8.0
HPC25/25E-M	360 # 40 # 0	0	815 # 245 [a]	0 # 0	640 # 190 [a]	175	8.0
HPC100/100E-M	360 # 40 # 0	0	0 # 980 [a]	0 # 0	0 # 760 [a]	210	8.0
SCC100/0M	300 # 0 # 0	340	0 # 0	0 # 530	940 # 0	185	6.5
SCC100/50M	300 # 0 # 0	340	0 # 0	0 # 530	475 # 435	210	6.5
SCC100/100M	300 # 0 # 0	340	0 # 0	0 # 530	0 # 865	235	6.5
SCC100/0M-G	0 # 0 # 425	340	0 # 0	0 # 430	940 # 0	185	6.5
SCC100/50M-G	0 # 0 # 425	340	0 # 0	0 # 430	475 # 435	210	6.5
SCC100/100M-G	0 # 0 # 425	340	0 # 0	0 # 430	0 # 865	235	6.5

[a] In these mixes, early-age RA was used in both the fine (0/4 mm) and coarse (4/22 mm) aggregate fractions.

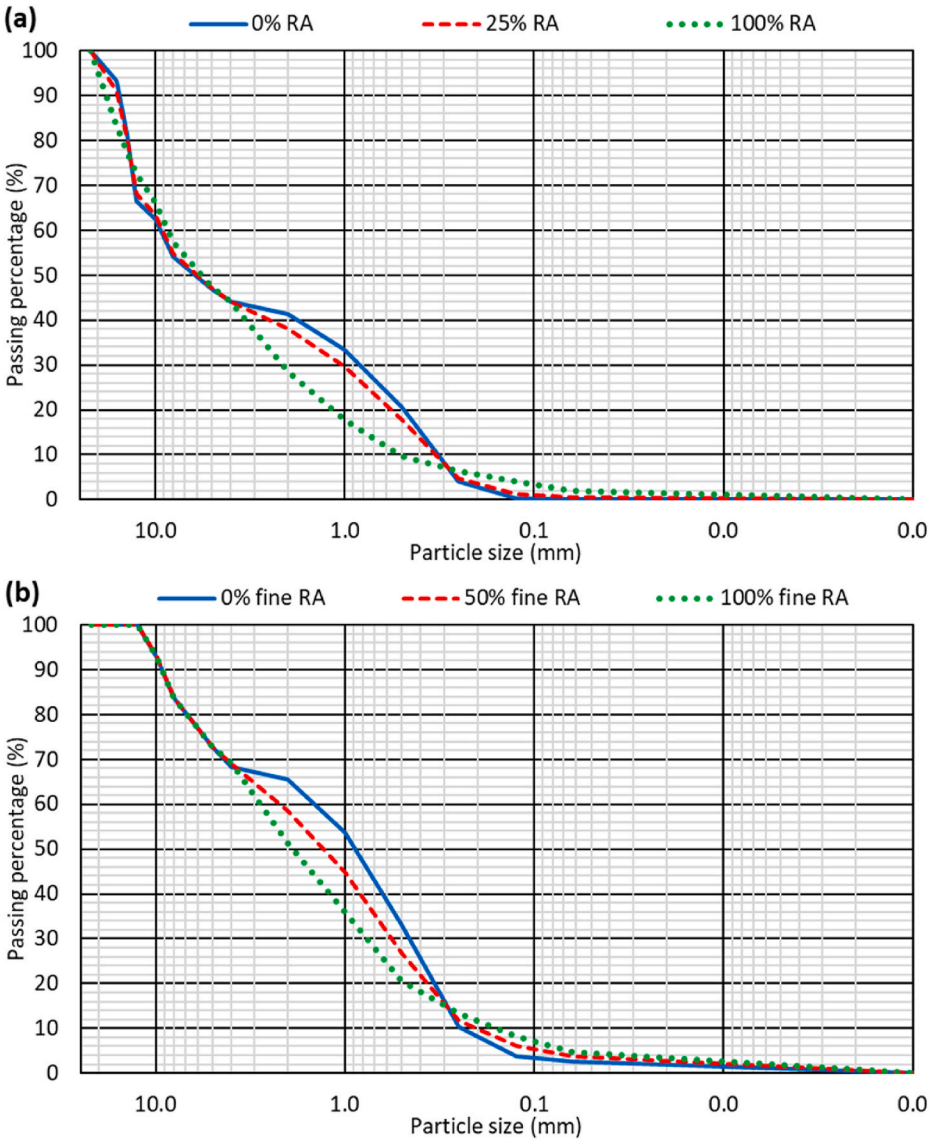

Fig. 2. Overall size distribution: (a) HPC mixes; (b) SCC mixes (SCC with OPC had almost the same overall size distribution than SCC with CEM III/A).

$$\varepsilon_{cd}(t) = -\frac{t-1}{(t-1)+0.04\times\sqrt{h_0^3}}\times k_h \times \varepsilon_{cd,0} \quad (1)$$

In the shrinkage-prediction formula of Eurocode 2, the involved variables are:

- t: time elapsed since concrete casting, *i.e.* concrete age, in days;
- h_0: average thickness of the section of the concrete element whose shrinkage is to be estimated, in mm. It is calculated as twice the area of the section of the concrete element divided by the atmosphere-contact perimeter of the section;
- k_h: dimensionless average-thickness-dependent coefficient. It takes the value of 1.00 for an average thickness of 100 mm; 0.85 for an average thickness of 200 mm; 0.75 for an average thickness of 300 mm; and 0.70 for average thicknesses higher than 500 mm. For average thicknesses between the indicated ones, a linear interpolation can be performed;
- $\varepsilon_{cd,0}$: initial drying shrinkage of concrete, in mm/m. It depends on the strength class of the concrete and the relative humidity to which the concrete element is exposed. Its value can be determined interpolating from Table 3.

2.4.2. US standard: ACI 209.2R

The US standard (ACI 209.2R [12]) considers as valid a shrinkage-prediction model developed in 1971. This model, shown in Equation (2), considers that total shrinkage (ε_{sh}, mm/m), sum of autogenous and drying shrinkage, evolves hyperbolically with time.

$$\varepsilon_{sh}(t,\ t_c) = -\frac{(t-t_c)^{\alpha}}{f+(t-t_c)^{\alpha}}\times \varepsilon_{shu} \quad (2)$$

The variables involved in estimating shrinkage through US standard are as follows:

- t: time elapsed since concrete casting, *i.e.* concrete age, in days;
- t_c: age of concrete at which its drying starts, in days. This instant in time can be considered the point at which concrete shrinkage begins. 1 day is usually adopted as the standard value;
- ε_{shu}: infinite-time shrinkage of concrete, in mm/m. Under a relative humidity of 40%, a value of 0.780 mm/m is considered. To adapt to other ambient conditions and the varying composition of concrete, this value is corrected by multiplying it by seven correction coefficients γ that depend on aspects such as the relative humidity, the moist-curing time, the cement content, or the proportion of fine aggregate (Table 4);
- α: dimensionless adjustment coefficient which is usually 1;
- f: adjustment coefficient that allows considering the shape and size of the concrete element whose shrinkage is to be estimated. It is calculated by Equation (3), in which V is the volume of the concrete element, in mm^3, and S, the surface area of the concrete element in contact with the atmosphere, in mm^2.

Table 3
Initial drying shrinkage of concrete ($\varepsilon_{cd,0}$, mm/m) of the Eurocode 2 shrinkage-prediction model [2].

$f_{ck,cylinder}/f_{ck,cube}$ [a] (MPa)	Relative humidity (%)					
	20	40	60	80	90	100
20/25	0.62	0.58	0.49	0.30	0.17	0.00
40/50	0.48	0.46	0.38	0.24	0.13	0.00
60/75	0.38	0.36	0.30	0.19	0.10	0.00
80/95	0.30	0.28	0.24	0.15	0.08	0.00
90/105	0.27	0.25	0.21	0.13	0.07	0.00

[a] To calculate the characteristic compressive strength of concrete (f_{ck}), 8 MPa are subtracted from the average strength of the concrete, which is the one experimentally measured; *"cylinder"* or *"cube"* refers to the considered specimen shape.

Table 4
Coefficients γ of ACI 209.2R model [12].

Coefficient	Formula	Independent variables
Moist-curing-time coefficient ($\gamma_{sh,tc}$)	$\gamma_{sh,tc} = 1.202 - 0.234 \times log(t_c)$	t_c: moist-curing time (days)
Ambient-relative-humidity coefficient ($\gamma_{sh,RH}$)	$\gamma_{sh,RH} = \begin{cases} 1.40 - 1.02\times h & if\ 0.40 \le h \le 0.80 \\ 3.00 - 3.0\times h & if\ 0.80 \le h \le 1.00 \end{cases}$	h: ambient relative humidity (percentage of one)
Size-specimen coefficient ($\gamma_{sh,vs}$)	$\gamma_{sh,vs} = 1.2\times exp\left(-0.00472\times V/S\right)$	V: volume of the specimen (mm^3) S: surface of the specimen (mm^2)
Slump coefficient ($\gamma_{sh,s}$)	$\gamma_{sh,tc} = 0.89 + 0.00161\times s$	s: slump (mm)
Fine-aggregate coefficient ($\gamma_{sh,\Psi}$)	$\gamma_{sh,\Psi} = \begin{cases} 0.30 + 0.014\times\Psi & if\ \Psi \le 50\% \\ 0.90 + 0.002\times\Psi & if\ \Psi > 50\% \end{cases}$	Ψ: ratio of fine aggregate to total aggregate by weight (percentage)
Cement-content coefficient ($\gamma_{sh,c}$)	$\gamma_{sh,c} = 0.75 + 0.00061\times c$	c: cement content (kg/m^3)
Air-content coefficient ($\gamma_{sh,\alpha}$)	$\gamma_{sh,\alpha} = 0.95 + 0.008\times\alpha \ge 1$	α: air content (percentage)

$$f = 26\times exp\left(0.0142\times\frac{V}{S}\right) \quad (3)$$

3. Results and discussion: experimental results

This section presents the experimental results necessary for the development of the proposed shrinkage-estimation model, which is addressed in the next section.

3.1. Fresh behaviour: slump and slump-flow tests

The fresh-state behaviour of the mixes is shown in Fig. 3. All mixes exhibited the required workability in the mix design: slump class S4 (HPC mixes) or slump-flow class SF3 (SCC mixes) as per EN 206 [50].

Concerning the HPC mixes (Fig. 3a), RA increased the internal friction of the mix, which was compensated by the water adjustment (Table 2) [60]. This also compensated for its higher water absorption [54], so that no outstanding negative effect of this waste on the slump was observed. Early-age RA, possibly more rounded in shape than matured RA, led to a slight increase in slump, around 1%. Finally, the use of 10% MgO reduced the workability mainly due to its more irregularly shaped particles than those of OPC [61], as well as its smaller particle size and decreased dragging capacity of the aggregate particles [42]. The interaction between the negative effects of RA and MgO led to a higher slump decrease the higher the RA content. For more information, a more detailed analysis of the workability of these HPC mixes can be found in another studies by the authors [34,46].

Unlike HPC, SCC is much more sensitive to the fines content [16], which explains the results shown in Fig. 3b. On the one hand, the addition of fine RA increased the slump flow, as the higher fines content of RA than that of NA (Fig. 1) compensated the irregular shape of this waste [55]. On the other, the lower dragging capacity of GGBFS, due to its higher grinding fineness than OPC's [41], was compensated by reducing the proportion of coarse aggregate, which even allowed increasing the slump flow. The SCC mixes also complied with the requirements of passing-ability and viscosity to be considered as SCC, according to the results in similar SCC mixes [62].

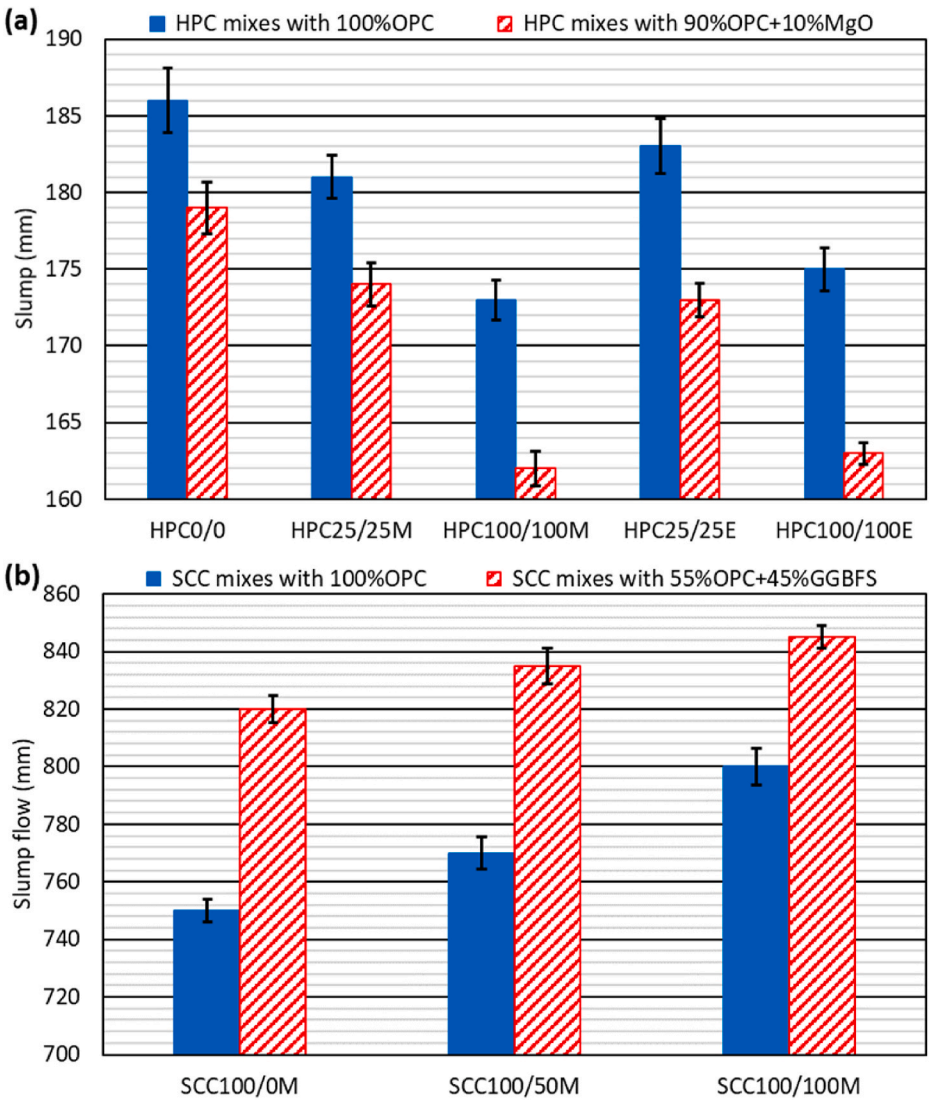

Fig. 3. Fresh tests: (a) slump test in HPC mixes; (b) slump-flow test in SCC mixes.

3.2. 28-day compressive strength

The 28-day compressive strength was measured on cubic specimens. The results obtained for all the mixes are shown in Fig. 4. Compressive-strength measurement was necessary to determine the initial drying shrinkage ($\varepsilon_{cd,0}$) of the shrinkage-prediction model of Eurocode 2 [2].

The reference HPC mix (100% OPC and NA) had a compressive strength of 74.1 MPa, which was affected by different factors (Table 5). A broad analysis of the compressive strength of these HPC mixes can be found elsewhere [34,46], the key aspects of their behaviour being the following:

- First, the strength decreased almost linearly when adding matured RA, so the mix HPC100/100M had a compressive strength of 61.4 MPa. This reduction in strength was due to the increase in porosity and the decrease in adhesion in the interfacial transition zones caused by this waste [27,55];
- The strength loss when adding early-age RA was slightly higher than that caused by RA, so that the mix HPC100/100E had a compressive strength of 57.4 MPa. As the parent concrete had a lower strength when producing early-age RA, HPC exhibited a lower compressive strength when RA of that maturity was used in its manufacture [63–65];
- Finally, the use of 10% MgO led to a 5–10 MPa decrease in compressive strength because magnesium hydroxide, obtained after MgO hydration, shows lower strength than calcium-silicate-hydrates, resulting from OPC hydration [42]. The presence of magnesium hydroxide also caused an expansion that could micro-crack the concrete and reduce the strength [45]. The strength loss was higher for greater RA content, possibly due to the greater increase in porosity when adding both products [46].

In SCC (Fig. 4b and Table 5), the use of 100% coarse RA allowed yielding a compressive strength higher than 50 MPa, suitable for structural use [2,3]. This strength also decreased linearly as the content of fine matured RA increased, so that the mix SCC100/100M had a strength of 35.3 MPa. Increasing the binder content when GGBFS was added enabled the compressive strength to increase by 4–10 MPa [41]. This strength gain was higher in the mixes with 100% fine RA, showing the good interaction between GGBFS and fine RA [66].

3.3. Shrinkage

The shrinkage of all the concrete mixes was evaluated from 1 to 91 days. The temporal evolution of shrinkage is shown in Fig. 5 for HPC and Fig. 6 for SCC.

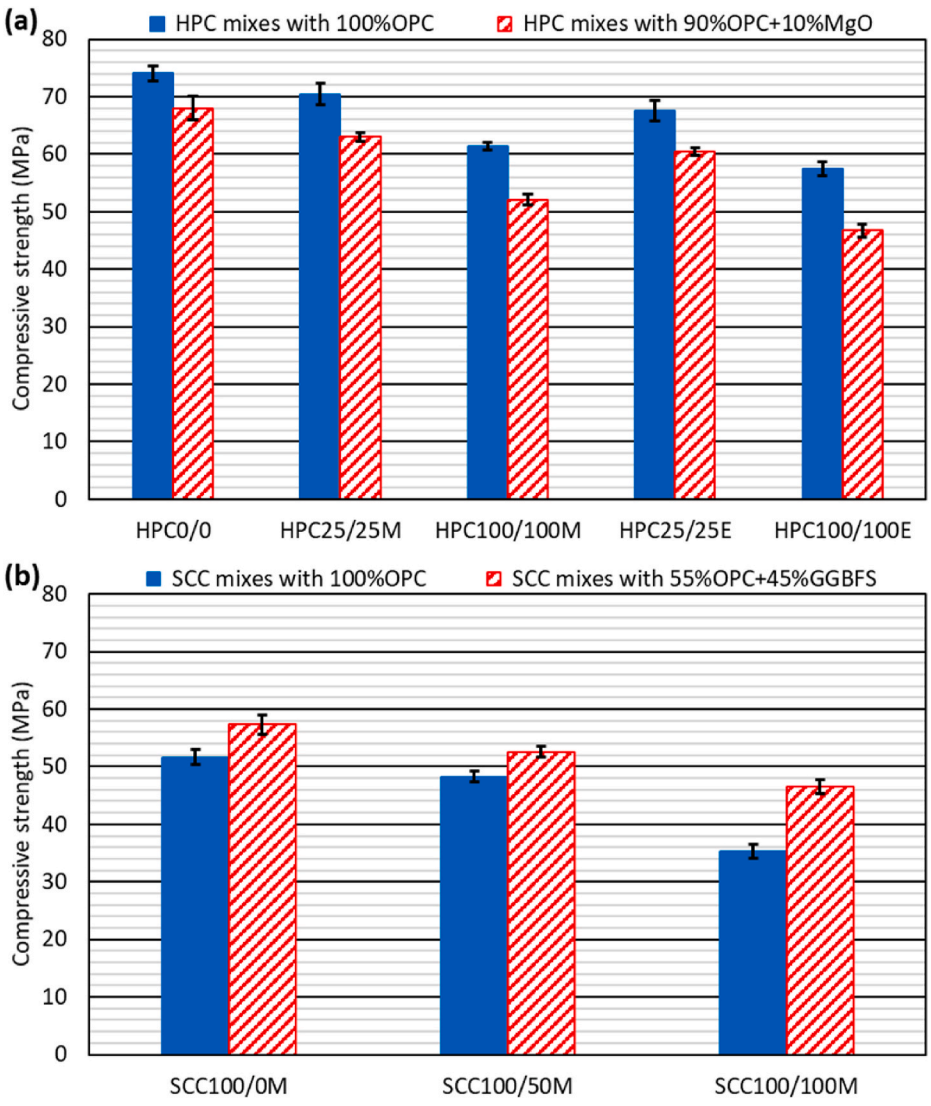

Fig. 4. 28-day compressive strength: (a) HPC mixes; (b) SCC mixes.

The shrinkage of HPC was affected by the same factors as the compressive strength (Table 6): the content of RA and its maturity, and the addition of MgO. An analysis of the shrinkage of these mixes in detail can be found in other papers [34,46], so only the results necessary for the adjustment of the proposed shrinkage-prediction model are reported here. The key aspects of the shrinkage behaviour of the HPC mixes were:

- Matured RA increased shrinkage, which doubled by adding 100% RA. Its higher water absorption, which increased the deferred water evaporation [33], and its lower stiffness, which reduced the opposition of the aggregate when the cementitious matrix contracted [11], explain these results;
- Early-age RA slightly increased shrinkage by 0.040–0.050 mm/m at 91 days compared to matured RA. RA has a rheological nature, as it comes from the crushing of a parent concrete [64], so it experiences shrinkage. Crushing of the parent concrete at 7 days made the obtained RA (early-age RA) experience higher shrinkage than when crushing the parent concrete six months after its casting (matured RA) [34]. This in turn led to a higher shrinkage in HPC;
- Finally, the expansion because of MgO hydration, shown by the length increase during the first days of the mixes made with this binder (Fig. 5b), allowed reducing shrinkage [43]. This decrease was 40% when 100% NA was used and around 30% when 100% matured RA was used, so the negative effects of RA explained before partially compensated the shrinkage reduction due to MgO expansion [46].

As expected, the SCC shrinkage was higher than that of HPC because of its higher proportion of fine aggregate [16]. The effect of each factor on 91-day shrinkage of SCC is shown in Table 6. The effect of RA on SCC was exactly the same as for HPC, as its lower stiffness and higher absorption of water than NA resulted in increased shrinkage (Fig. 6) [11]. GGBFS reduced shrinkage compared to OPC, as the literature shows for vibrated concrete [38,41]. This was due to the more compact micro-structure of the cementitious matrix that the higher grinding fineness of GGBFS allows creating [41], and was indifferent to the reduction of the amount of coarse aggregate required to reach a high slump flow when using it. This shrinkage improvement due to GGBFS was reduced when increasing the content of fine RA, like the effect of MgO on HPC, possibly due to the lower opposition of RA when the cementitious matrix contracted [59].

4. Model development

In this section, the proposed shrinkage-prediction model is explained. Simultaneously, to exemplify the model, it is fitted for the 16 studied mixes through the experimental results discussed in the previous

Table 5
Factor effect on 28-day compressive strength.

Mix	28-day compressive strength (MPa)	Variation due to MgO addition (%)	Variation due to CEM III/A addition (%)	Variation due to RA addition (%)	Variation due to fine RA addition (%)	Variation due to RA's maturity (%)
HPC0/0	74.1	0.0	0.0	0.0	0.0	0.0
HPC25/25M	70.4	0.0	0.0	−5.0	0.0	0.0
HPC100/100M	61.4	0.0	0.0	−17.2	0.0	0.0
HPC25/25E	67.5	0.0	0.0	−9.0	0.0	−4.2
HPC100/100E	57.4	0.0	0.0	−22.6	0.0	−6.5
HPC0/0-M	68.0	−8.2	0.0	0.0	0.0	0.0
HPC25/25M-M	63.0	−10.5	0.0	−7.4	0.0	0.0
HPC100/100M-M	52.1	−15.1	0.0	−23.4	0.0	0.0
HPC25/25E-M	60.4	−10.6	0.0	−11.8	0.0	−4.1
HPC100/100E-M	46.7	−18.6	0.0	−31.3	0.0	−10.4
SCC100/0M	51.6	0.0	0.0	0.0	0.0	0.0
SCC100/50M	48.3	0.0	0.0	0.0	−6.4	0.0
SCC100/100M	35.3	0.0	0.0	0.0	−31.6	0.0
SCC100/0M-G	57.3	0.0	+11.0	0.0	0.0	0.0
SCC100/50M-G	52.6	0.0	+8.9	0.0	−8.2	0.0
SCC100/100M-G	46.6	0.0	+32.0	0.0	−18.7	0.0

Variations in 28-day compressive strength calculated with respect to the mixes with exactly the same composition but without the analysed composition modification (MgO and RA addition and use of early-age RA for the HPC mixes; and use of CEM III/A and fine RA addition for the SCC mixes).

section.

4.1. Analysis of shrinkage-prediction models from standards

Fig. 7 shows for the 16 studied concrete mixes the comparison between the experimental shrinkage values and those estimated through the Eurocode 2 (Equation (1)) and ACI 209.2R (Equation (2)) models [2,12]. It can be noted that the overall fit was not adequate for both, with a deviation of ±20% being exceeded in many cases. The Eurocode 2 model showed a better overall accuracy.

On the other hand, it was analysed whether the temporal evolution of shrinkage in recycled aggregate concrete coincided with that shown by the models. For that purpose, the Eurocode 2 and ACI 209.2R models [2,12] were adapted with variable coefficients, introducing the correction coefficients A, B and C in each of them, as shown in Equation (4) and Equation (5), respectively. A mix-by-mix multiple-regression adjustment, disregarding the positive shrinkage values caused by MgO expansion, allowed calculating for each mix the values of the correction coefficients A, B and C, and the coefficient R^2, higher than 95% in all cases (Table 7). Therefore, both models were able to optimally fit and predict the shrinkage of all recycled aggregate concrete mixes. For it, the only modification necessary in the models was the introduction of correction coefficients, as the temporal trend of the shrinkage shown by the models was already valid for this type of concrete. Nevertheless, the usefulness of these correction coefficients A, B and C is low, as they are different for each mix, which implies that the model to be used for shrinkage estimation is different for mixes with a different alternative binder or RA content, and, therefore, no model generalisation can be made.

$$\varepsilon_{cd}(t) = -\frac{A \times (t-1)}{B \times (t-1) + C \times 0.04 \times \sqrt{h_0^3}} \times k_h \times \varepsilon_{cd,0} \quad (4)$$

$$\varepsilon_{sh}(t,\ t_c) = -\frac{A \times (t-t_c)^{\alpha}}{B \times f + C \times (t-t_c)^{\alpha}} \times \varepsilon_{shu} \quad (5)$$

4.2. Analysis of concrete-age-dependent simple regression

Another possibility to estimate concrete shrinkage is to perform a mix-by-mix simple regression as a function of concrete age, *i.e.* considering concrete age (t, in days) as the independent variable and shrinkage (ε, in mm/m) as the dependent variable. A statistical analysis of maximization of the coefficient R^2 showed that the simple-regression model that is best adjusted to the temporal evolution of shrinkage was the logarithmic one, which is shown in Equation (6). The adjustment of this model to all the mixes (calculation of coefficients D and E), which is shown in Table 8, was adequate, obtaining in this case also coefficients R^2 always higher than 95%. However, these coefficients lack practical usefulness, since they are different for each type of mix prepared with different binders and RA contents, so the model to be used for each mix is also different. This situation is the same as that regarding the adjustment of Equation (4) and Equation (5) shown in the previous section (Table 7).

$$\varepsilon = -D \times ln(t) + E \quad (6)$$

4.3. Partial correction coefficients: concept and usefulness

Partial coefficients, for example of load increase or strength reduction, are commonly used in the design of concrete structures [8]. The partial coefficients are for correction when they are used to adapt a property-estimation formula to the composition or characteristics of every concrete mix [67]. Without going any further, the shrinkage-prediction models of the standards use partial correction coefficients, Eurocode 2 [2] by means of the k_h coefficient (Equation (1)) and ACI 209.2R [12] through the seven coefficients γ (Table 4).

As evidenced by the high coefficients R^2 obtained (Table 7), the use of multiplicative correction coefficients (Equation (4), Eurocode 2; and Equation (5), ACI 209.2R) to predict the concrete shrinkage when adding recycled aggregate and different alternative binders is valid. However, for generalization and simplification of the model to be possible, the introduced coefficient has to be common to the whole model (formula), unlike Equation (4) and Equation (5), and a different

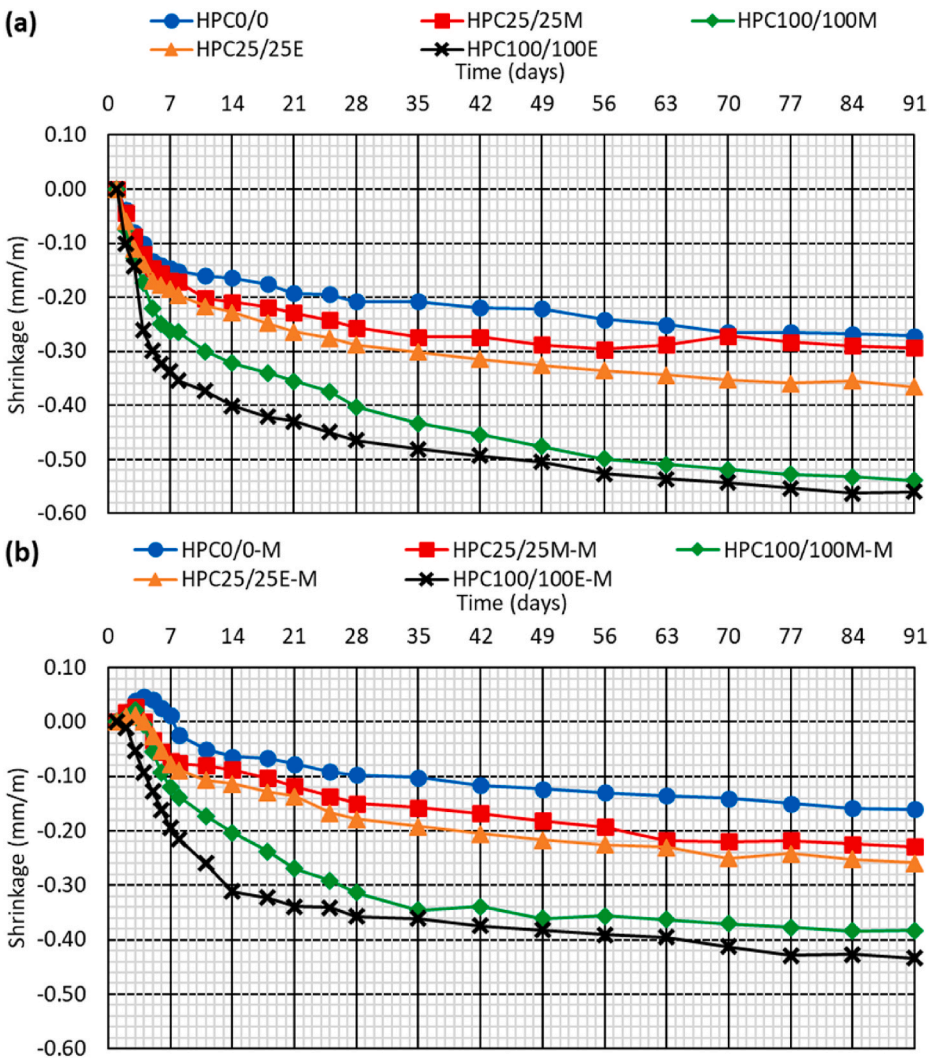

Fig. 5. Shrinkage of HPC: (a) mixes with 100% OPC; (b) mixes with 90% OPC and 10% MgO.

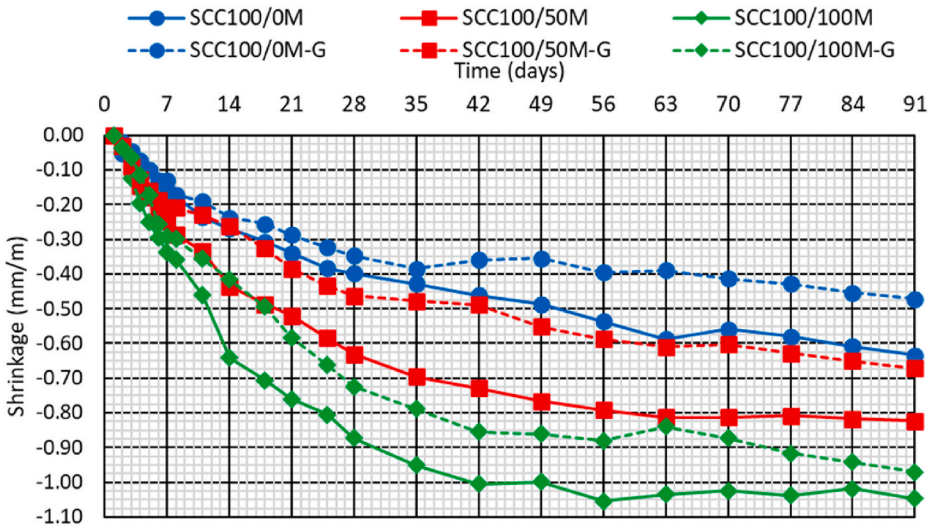

Fig. 6. Shrinkage of SCC.

coefficient should not be considered for each term of the formula. Therefore, a single partial multiplicative correction coefficient has to be considered. This coefficient can be determined by statistically adjusting the experimental shrinkage (ε_{exp}, mm/m) to the shrinkage estimated by those models (ε_{est}, mm/m) assuming a single partial correction coefficient C^y (Equation (7)).

Table 6
Factor effect on 91-day shrinkage.

Mix	91-day shrinkage (mm/m)	Standard deviation (mm/m)	Variation due to MgO addition (%)	Variation due to CEM III/A addition (%)	Variation due to RA addition (%)	Variation due to fine RA addition (%)	Variation due to RA's maturity (%)
HPC0/0	−0.271	0.022	0.0	0.0	0.0	0.0	0.0
HPC25/25M	−0.293	0.012	0.0	0.0	+8.1	0.0	0.0
HPC100/100M	−0.539	0.007	0.0	0.0	+98.7	0.0	0.0
HPC25/25E	−0.366	0.026	0.0	0.0	+34.8	0.0	+24.8
HPC100/100E	−0.559	0.011	0.0	0.0	+106.2	0.0	+3.8
HPC0/0-M	−0.160	0.033	−40.9	0.0	0.0	0.0	0.0
HPC25/25M-M	−0.229	0.018	−21.8	0.0	+43.1	0.0	0.0
HPC100/100M-M	−0.383	0.028	−29.0	0.0	+139.0	0.0	0.0
HPC25/25E-M	−0.258	0.027	−29.3	0.0	+61.3	0.0	+12.7
HPC100/100E-M	−0.434	0.036	−22.4	0.0	+171.1	0.0	+13.4
SCC100/0M	−0.634	0.052	0.0	0.0	0.0	0.0	0.0
SCC100/50M	−0.823	0.073	0.0	0.0	0.0	+29.7	0.0
SCC100/100M	−1.047	0.075	0.0	0.0	0.0	+65.0	0.0
SCC100/0M-G	−0.472	0.018	0.0	−25.7	0.0	0.0	0.0
SCC100/50M-G	−0.672	0.055	0.0	−18.4	0.0	+42.5	0.0
SCC100/100M-G	−0.971	0.057	0.0	−7.3	0.0	+105.8	0.0

Variations in 91-day shrinkage calculated with respect to the mixes with exactly the same composition but without the analysed composition modification (MgO and RA addition and use of early-age RA for the HPC mixes; and use of CEM III/A and fine RA addition for the SCC mixes).

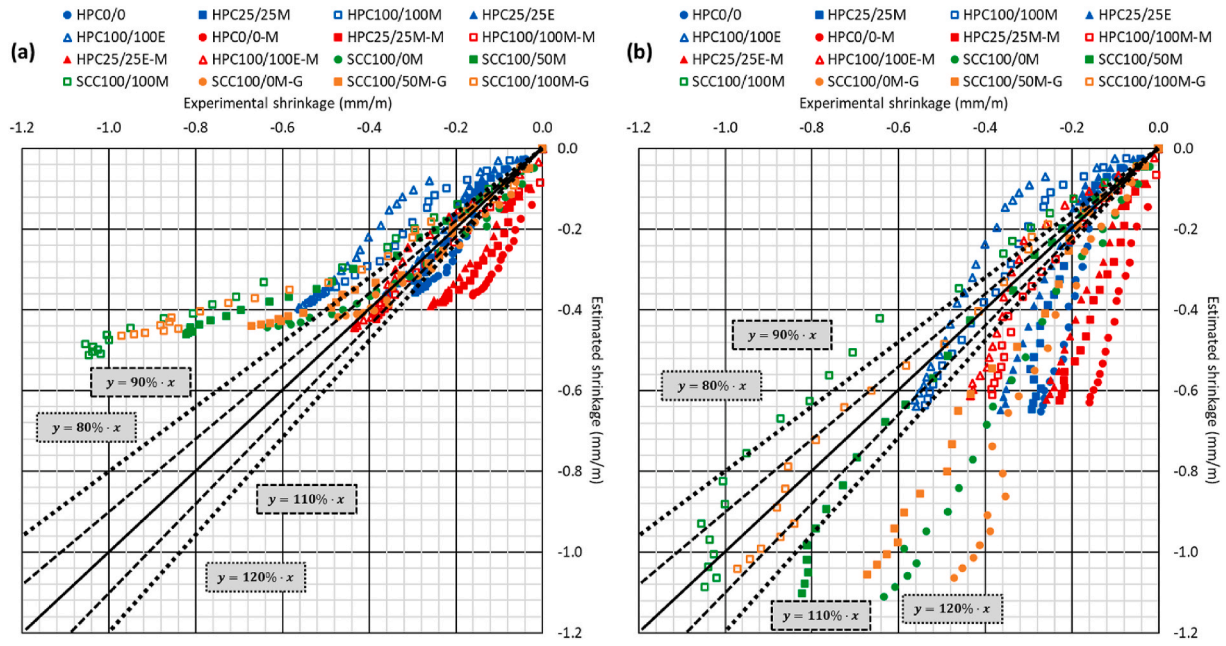

Fig. 7. Comparison of experimental shrinkage and shrinkage estimated through: (a) Eurocode 2 model [2]; (b) ACI 209.2R model [12].

$$\varepsilon_{exp} = C^{y} \times \varepsilon_{est} \quad (7)$$

A partial correction coefficient has to be considered for each modification in the composition of concrete. For instance, in the mixes of this research work, there will be a partial correction coefficient depending on the concrete type (HPC or SCC), depending on the RA content, the RA's maturity, and the binder type (OPC, GGBFS, or reactive MgO). It is also necessary to consider shrinkage-prediction interactions between those composition features, as, for example, the effect of a binder on concrete shrinkage can vary depending on the amount of RA [47]. These interactions can be detected by calculating the partial correction coefficient for every modification in the concrete composition without considering the rest of modifications. If coefficients R^2 below 70% are obtained in this way, according to the experience of the authors it is likely that interactions between the different composition modifications have to be considered. Finally, a correction coefficient should also be introduced depending on whether the age of concrete is less or more

Table 7
Mix-by-mix multiple-regression fitting of Eurocode 2 and ACI 209.2R shrinkage models [2,12] expressed with variable coefficients.

Mix	Eurocode 2 model				ACI 209.2R model			
	A	*B*	*C*	R^2 (%)	*A*	*B*	*C*	R^2 (%)
HPC0/0	0.597	0.895	0.354	95.44	0.246	0.132	0.856	95.59
HPC25/25M	0.335	0.452	0.165	98.90	0.228	0.120	0.833	98.90
HPC100/100M	0.129	0.108	0.052	97.54	0.104	0.037	0.165	97.49
HPC25/25E	0.754	0.858	0.374	97.88	0.444	0.183	1.180	97.97
HPC100/100E	1.155	0.946	0.294	98.08	0.092	0.018	0.146	98.08
HPC0/0-M	0.154	0.293	0.772	98.74	0.962	4.004	3.776	98.87
HPC25/25M-M	0.116	0.167	0.355	96.79	0.656	1.499	1.920	98.21
HPC100/100M-M	0.088	0.090	0.111	97.07	0.082	0.072	0.147	97.07
HPC25/25E-M	0.091	0.128	0.211	98.68	0.262	0.459	0.709	98.68
HPC100/100E-M	0.088	0.096	0.062	98.60	0.078	0.036	0.142	98.60
SCC100/0M	0.272	0.166	0.492	99.56	0.206	0.323	0.391	99.56
SCC100/50M	0.079	0.039	0.077	99.65	0.202	0.164	0.295	99.65
SCC100/100M	0.126	0.056	0.090	98.87	0.197	0.103	0.229	98.87
SCC100/0M-G	0.181	0.161	0.270	98.67	0.216	0.286	0.608	98.67
SCC100/50M-G	0.170	0.102	0.240	98.93	0.224	0.263	0.400	98.93
SCC100/100M-G	0.112	0.048	0.109	98.97	0.215	0.162	0.256	98.97

Table 8
Mix-by-mix concrete-age-dependent simple-regression adjustment of experimental shrinkage.

Mix	*D*	*E*	R^2 (%)
HPC0/0	0.056	−0.021	97.42
HPC25/25M	0.064	−0.029	95.93
HPC100/100M	0.119	−0.009	99.40
HPC25/25E	0.078	−0.025	99.04
HPC100/100E	0.115	−0.071	95.55
HPC0/0-M	0.053	0.083	99.24
HPC25/25M-M	0.066	0.073	97.92
HPC100/100M-M	0.118	0.114	96.55
HPC25/25E-M	0.076	0.081	98.90
HPC100/100E-M	0.106	0.022	96.48
SCC100/0M	0.158	0.120	96.75
SCC100/50M	0.219	0.131	97.74
SCC100/100M	0.282	0.144	96.66
SCC100/0M-G	0.110	0.049	97.67
SCC100/50M-G	0.162	0.095	97.30
SCC100/100M-G	0.252	0.172	96.70

than 7 days in order to get an accurate shrinkage estimation at early ages.

It should also be noted that in the event that a low accuracy of the model is obtained by using a single partial correction coefficient as shown in Equation (7) and considering shrinkage-prediction interactions, it is advisable to consider a combined partial correction coefficient in which a logarithmic dependence on concrete age (*t*, days) is included, as shown in Equation (8) and Equation (9). The introduction of the logarithmic dependence on concrete age allows a more accurate representation of the mechanisms by which each alternative raw material affects concrete shrinkage, and, therefore, a more precise shrinkage prediction. The choice of one of the two options shown in Equation (8) and Equation (9) will depend on the precision of the adjustment. The authors' experience suggests that the use of a combined partial correction coefficient is recommended when the use of a partial correction coefficient as shown in Equation (7) provides coefficients R^2 below 70%. This modification significantly increases the accuracy of the adjustment in such cases, enabling coefficients R^2 of up to 92–98% to be reached, since, as shown in section 4.2, the optimal simple regression of shrinkage as a function of time is logarithmic in nature.

$$\varepsilon_{exp} = (C^{y} \times ln(t)) \times \varepsilon_{est} \tag{8}$$

$$\varepsilon_{exp} = \left(\frac{C^{y}}{ln(t)}\right) \times \varepsilon_{est} \tag{9}$$

4.4. Model adjustment: values of partial correction coefficients

Considering the aspects discussed in section 4.3, the partial correction coefficients for estimating the shrinkage of the mixes analysed in this study are shown below.

4.4.1. HPC mixes

The HPC mixes were prepared with different contents (0%, 25%, and 100%) of RA, simultaneously adding the coarse and fine fractions of this waste. In addition, RA of two different maturities was used, early-age RA (parent concrete crushed one week after casting) and matured RA (parent concrete crushed six months after casting). Finally, 10% reactive MgO was added as an alternative binder. According to these aspects, the shrinkage of the HPC mixes is estimated by Equation (10).

$$\varepsilon_{HPC} = \varepsilon_{est} \times C^{HPC} \times C^{cRA} \times C^{mRA} \times C^{MgO} \times C^{t} \tag{10}$$

In Equation (10), the terms involved are:

- ε_{HPC}: shrinkage (mm/m) of the HPC mix;
- ε_{est}: estimated shrinkage (mm/m) of the HPC mix using Eurocode 2 and ACI 209.2R models [2,12];
- C^{HPC}: partial correction coefficient for adapting the shrinkage-prediction models of the standards, developed for conventional vibrated concrete, to HPC;
- C^{cRA}: partial correction coefficient as a function of the RA amount. As both coarse and fine RA were simultaneously added, this coefficient reflects the effect of using both RA fractions at the same time;
- C^{mRA}: partial correction coefficient reflecting the effect of RA's maturity on shrinkage;
- C^{MgO}: partial correction coefficient showing the effect of adding 10% MgO on HPC shrinkage. Positive shrinkage (expansion) values at early ages caused by MgO were not considered for its calculation;
- C^{t}: concrete-age-dependent partial correction coefficient to improve the accuracy of the estimation when the age of HPC is less than 7 days.

The partial correction coefficients of the HPC mixes for both the Eurocode 2 [2] and ACI 209.2R [12] shrinkage-prediction models are shown in Table 9. Since the estimated shrinkage was different for both models (Fig. 7), the partial correction coefficients were also different. These coefficients mostly depended only on the RA content, which shows that the prediction interactions basically depended on the amount of RA, so that an equation of the same nature (reciprocal equation) was always obtained. The exception was the MgO partial correction coefficient C^{MgO} for the Eurocode 2 model, which not only depended on the RA content, but also on its maturity, thus a double interaction existed in

Table 9
Partial correction coefficients for HPC mixes.

Coefficient	Eurocode 2 model [2]	ACI 209.2R model [12]
C^{HPC}	0.810	$1.813/ln(t)$
C^{cRA}	$1/(0.998 - 0.433 \times RA)$	$1/(0.987 - 0.496 \times RA)$
C^{mRA}	$\begin{cases} 1 & \text{if matured RA} \\ 1.112 & \text{if early} - \text{age RA} \end{cases}$	$\begin{cases} 1 & \text{if matured RA} \\ 1.143 & \text{if early} - \text{age RA} \end{cases}$
C^{MgO}	$\begin{cases} 1 & \text{if 100\% OPC} \\ 0.122 \times ln(t) & \text{if 10\% MgO and 0\% RA} \\ 0.605 & \text{if 10\% MgO and matured RA} \\ 1/(0.941 + 0.599 \times RA) & \text{if 10\% MgO and early} - \text{age RA} \end{cases}$	$\begin{cases} 1 & \text{if 100\% OPC} \\ 1/(6.832 - 2.110 \times RA) & \text{if 10\% MgO} \end{cases}$
C^{t}	$\begin{cases} 1.512 & \text{if } t \leq 7 \text{ days and 100\% OPC} \\ 1 & \text{in other cases} \end{cases}$	$\begin{cases} 1.512 & \text{if } t \leq 7 \text{ days and 10\% MgO} \\ 1 & \text{in other cases} \end{cases}$

RA: content of RA of concrete (percentage per one); *t*: age of concrete (days).

this case.

4.4.2. SCC mixes

All the SCC mixes were made with 100% coarse RA. In addition, three fine RA contents were considered (0%, 50%, and 100%) and half of the mixes were made with CEM III/A (45% GGBFS). According to these aspects, the shrinkage of the SCC mixes is estimated by Equation (11).

$$\varepsilon_{SCC} = \varepsilon_{est} \times C^{SCC,100} \times C^{cfRA} \times C^{GGBFS} \times C^{t} \quad (11)$$

The terms involved in Equation (11) are:

- ε_{SCC}: shrinkage (mm/m) of the SCC mix;
- ε_{est}: estimated shrinkage (mm/m) of the SCC mix through Eurocode 2 and ACI 209.2R shrinkage-prediction models [2,12];
- $C^{SCC,100}$: partial correction coefficient for adapting the shrinkage-prediction models of the standards, developed for conventional vibrated concrete, to SCC manufactured with 100% coarse RA;
- C^{cfRA}: partial correction coefficient as a function of the content of fine RA;
- C^{GGBFS}: partial correction coefficient showing the effect of using CEM III/A (45% GGBFS) on SCC shrinkage;
- C^{t}: concrete-age-dependent partial correction coefficient to get an accurate estimation of SCC shrinkage at ages less than 7 days.

The partial correction coefficients for the SCC mixes are shown in Table 10. Again, as for the HPC mixes, different coefficients were obtained for both shrinkage-prediction models, and they are easier to apply in the ACI 209.2R model [12]. This was because, when adding different types of binders, no prediction interaction was found between the binder and the RA content, an aspect that did occur for the Eurocode 2 model [2]. Furthermore, in the Eurocode 2 model the type of binder also affected the partial correction coefficient as a function of the concrete age C^{t}.

4.5. Accuracy of the model

As shown in Fig. 8, the use of the shrinkage-prediction models of Eurocode 2 [2] and ACI 209.2R [12] modified by partial correction coefficients allowed estimating shrinkage at all ages with a maximum deviation of ±20%. The more outstanding fitting problems were encountered at early ages (smallest shrinkage values), which even led to the use of the coefficient C^{t}, as explained in the previous sections. However, the accuracy of the model increased with the age of concrete, so for shrinkages higher than 0.15 mm/m in absolute value the estimation was accurate and adjusted in practically all cases to a maximum deviation of ±20%. In fact, shrinkage at 91 days could be estimated with an accuracy of ±10% in 88% of the cases regardless of the model (Fig. 9). This shows the practical feasibility of using partial correction coefficients to estimate shrinkage, since in design tasks it is of particular interest to determine the shrinkage in the long-term [48].

4.6. Validation of the model

Two processes were used to check the validity of the proposed shrinkage-prediction procedure and of the partial correction coefficients obtained:

- On the one hand, it was checked whether the calculated partial correction coefficients were valid for estimating the shrinkage at ages over 90 days of similar mixes found in the literature (high-performance or self-compacting concretes with RA and MgO or GGBFS) [23,33,43,64,68,69]. Long-term shrinkage was considered because it is the most relevant shrinkage value in structural design [2,3]. As shown in Fig. 10, long-term shrinkage was estimated with maximum deviations of ±10% in 70% of the cases, while in the rest it was fitted to a maximum deviation of ±20%;
- On the other hand, as the number of studies with similar mixes for validation was not high, a validation based on modifying the initial

Table 10
Partial correction coefficients for SCC mixes.

Coefficient	Eurocode 2 model [2]	ACI 209.2R model [12]
$C^{SCC,100}$	$0.319 \times ln(t)$	0.567
C^{cfRA}	$\begin{cases} 1 & \text{if 0\% fine RA} \\ \sqrt{0.918 + 38.448 \times \sqrt{fRA}}/ln(t) & \text{in other cases} \end{cases}$	$\begin{cases} 1 & \text{if 0\% fine RA} \\ \sqrt{0.841 + 2.660 \times \sqrt{fRA}} & \text{in other cases} \end{cases}$
C^{GGBFS}	$\begin{cases} 1 & \text{if 100\% OPC} \\ 0.817 & \text{if 45\% GGBFS and 0\% fine RA} \\ 0.228 \times ln(t) & \text{in other cases} \end{cases}$	$\begin{cases} 1 & \text{if 100\% OPC} \\ 0.822 & \text{if 45\% GGBFS} \end{cases}$
C^{t}	$\begin{cases} 0.753 & \text{if } t \leq 7 \text{ days and 100\% OPC} \\ 1.397 & \text{if } t \leq 7 \text{ days and 45\% GGBFS} \\ 1 & \text{if } t > 7 \text{ days} \end{cases}$	$\begin{cases} 1.512 & \text{if } t \leq 7 \text{ days} \\ 1 & \text{if } t > 7 \text{ days} \end{cases}$

fRA: content of fine RA of concrete mix (percentage per one); *t*: age of concrete (days).

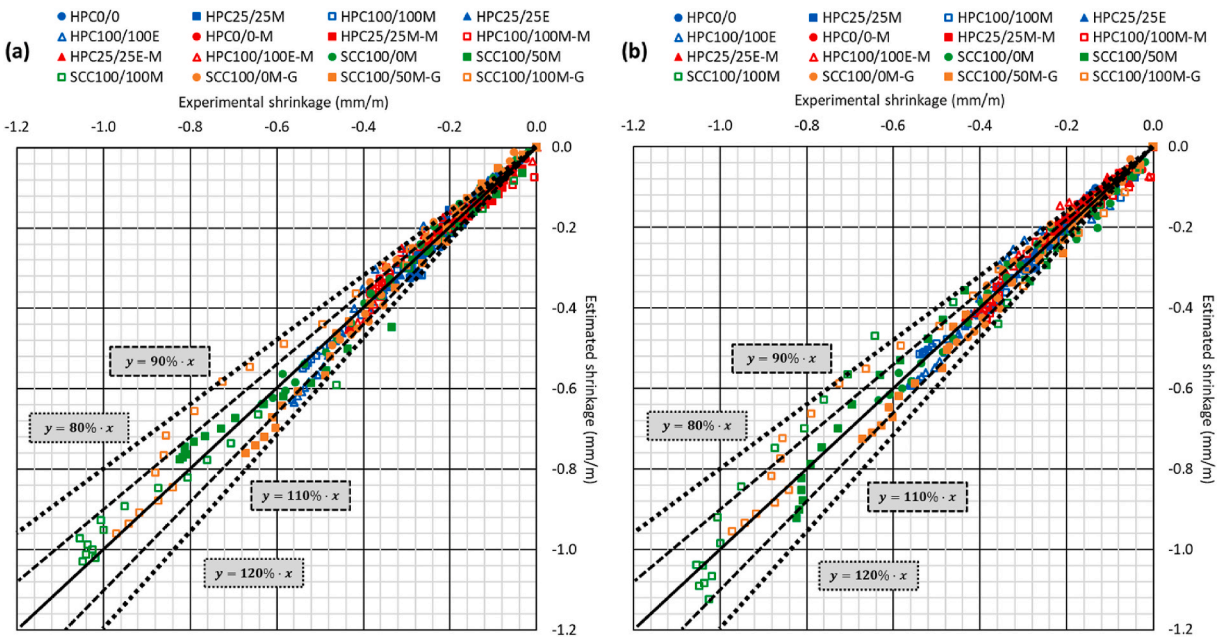

Fig. 8. Comparison of experimental shrinkage and shrinkage estimated through the partial correction coefficients for the (a) Eurocode 2 model [2]; (b) ACI 209.2R model [12].

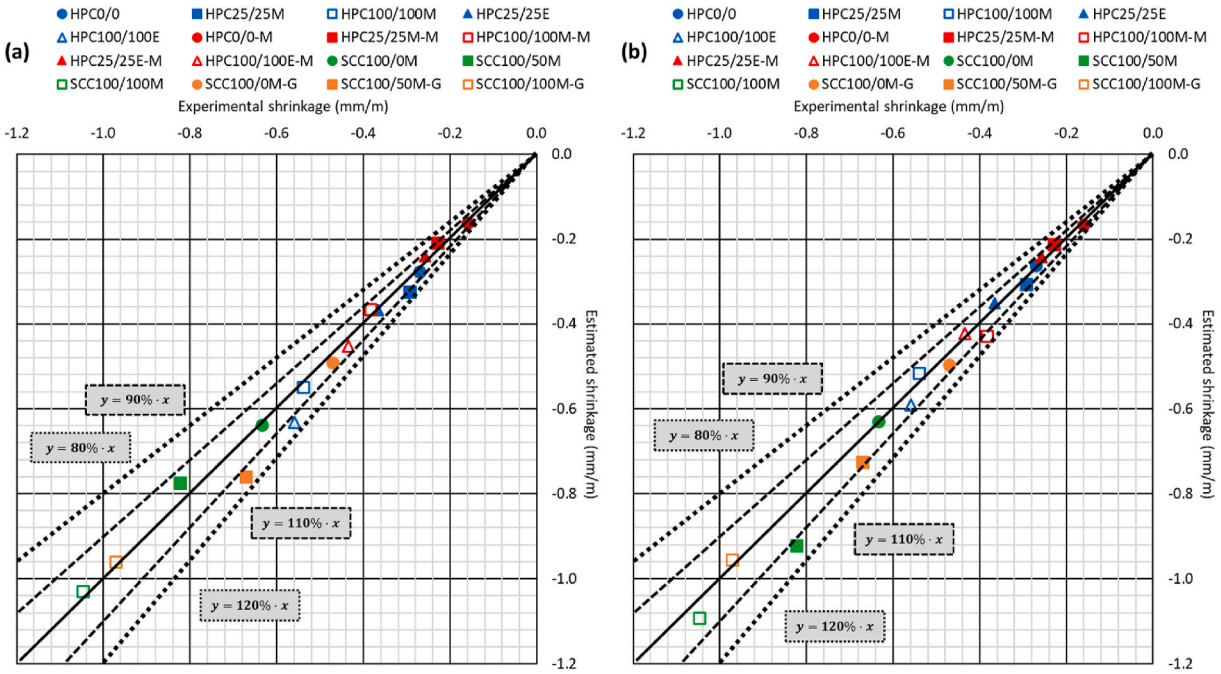

Fig. 9. Comparison of 91-day experimental shrinkage and shrinkage estimated through partial correction coefficients for: (a) Eurocode 2 model [2]; (b) ACI 209.2R model [12].

data for the model development was performed. This validation is commonly conducted when constructing models to predict some properties of concrete [70]. Thus, the partial correction coefficients were calculated with only 60% of the mixes. This calculation was carried out several times, different mixes being considering each time. The same partial correction coefficients were always obtained.

According to both validations performed, the proposed procedure based on the use of partial correction coefficients was valid and reliable for estimating the shrinkage of recycled aggregate concrete with any binder. Furthermore, the calculated partial correction coefficients would be valid for recycled aggregate high-performance concrete with MgO and recycled aggregate self-compacting concrete with GGBFS.

5. Conclusions

The shrinkage behaviour of recycled aggregate concrete has been analysed in this article. It has been found that the addition of recycled aggregate (RA) increases the shrinkage of both high-performance and self-compacting concrete, the shrinkage of the latter being higher. However, the use of alternative binders reduces shrinkage due to their expansive properties (magnesium oxide, MgO) or their higher grinding

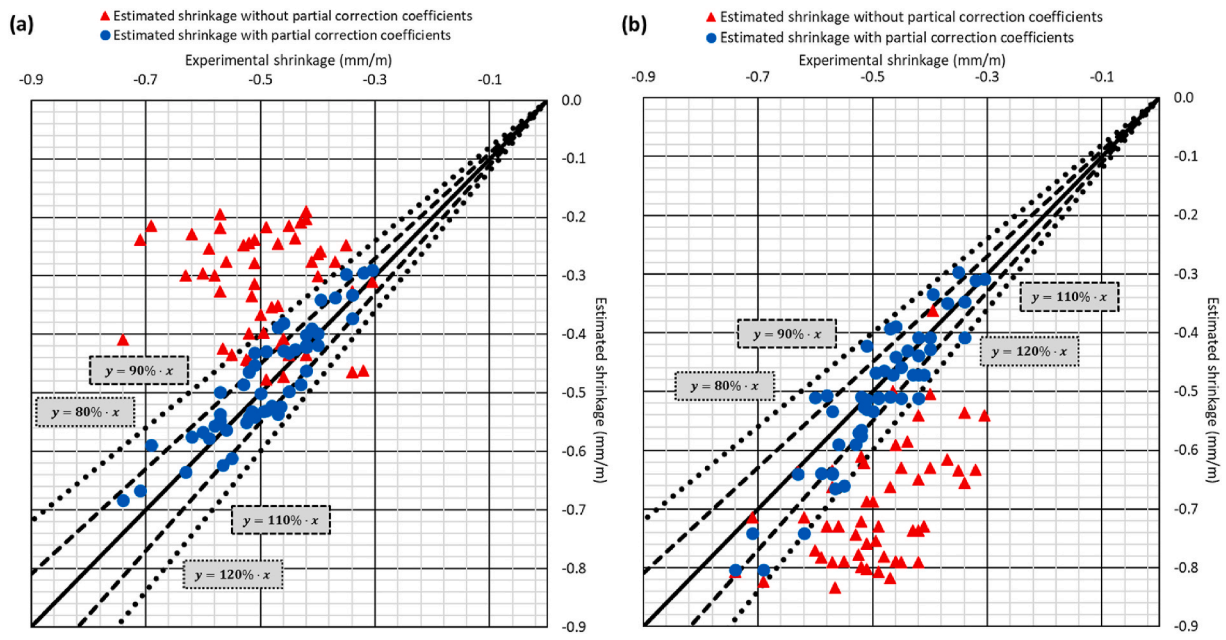

Fig. 10. Validation through existing studies [23,33,43,64,68,69] of the shrinkage-prediction partial correction coefficients for: (a) Eurocode 2 model [2]; (b) ACI 209.2R model [12].

fineness (ground granulated blast furnace slag, GGBFS). Furthermore, it has been demonstrated that the shrinkage of concrete when adding recycled aggregate can be estimated by partial correction coefficients. The following conclusions can be drawn from the proposed procedure for shrinkage estimation:

- Partial correction coefficients allow estimating the shrinkage of concrete with recycled aggregate using either Eurocode 2 [2] or ACI 209.2R [12] shrinkage-prediction model. Maximum deviations of ±10% for 91-day shrinkage were obtained for the mixes from both this study and the bibliography;
- A partial correction coefficient should be used for every change in concrete composition: type of concrete (vibrated, high-performance, or self-compacting), RA content, RA's maturity, and added alternative binder. Prediction interactions between these aspects should also be considered in these coefficients, as well as a concrete-age-dependent coefficient to get accurate estimates at early ages;
- The partial correction coefficients are numbers by which to multiply the shrinkage estimated through the standards [2,12]. However, when the estimation accuracy in this way is low, multiplying or dividing by the natural logarithm of concrete age leads to more precise estimations;
- The initially estimated shrinkage, as well as the prediction interactions between the factors affecting shrinkage, are different for each shrinkage-prediction model, Eurocode 2 [2] or ACI 209.2R [12]. Thus, the value and the conditions of use of the partial correction coefficients are also different for each model. The use of partial correction coefficients in the ACI 209.2R [12] shrinkage-prediction model is easier, as it has fewer relevant prediction interactions, so this model is recommended for predicting the shrinkage of recycled aggregate concrete.

The shrinkage-prediction procedure described is useful for a precise estimation of the shrinkage of concrete when adding recycled aggregate, although in this paper only the partial correction coefficients for high-performance and self-compacting concrete made with RA of different maturity, MgO, and GGBFS are provided (Tables 9 and 10). The next step in the research could be to obtain the partial correction coefficients for RA of different quality or with different amount of adhered mortar, as well as for the many alternative binders that can be used in recycled aggregate concrete. In this way, a database of partial correction coefficients could be created to standardise the shrinkage calculation in this type of concrete.

Declaration of competing interest

The authors declare that they have no known competing financial interests or personal relationships that could have appeared to influence the work reported in this paper.

Acknowledgements

This work was supported by the Spanish Ministry of Universities, MICINN, AEI, EU and ERDF [grant numbers PID2020-113837RB-I00; 10.13039/501100011033; FPU17/03374; EST19/00263]. Moreover, the authors acknowledge the support of the Junta de Castilla y León [grant number UIC231]; the University of Burgos [grant number Y135.GI]; and the Foundation for Science and Technology, CERIS Research Centre and Instituto Superior Técnico.

References

[1] V. Revilla-Cuesta, M. Skaf, J.A. Chica, J.A. Fuente-Alonso, V. Ortega-López, Thermal deformability of recycled self-compacting concrete under cyclical temperature variations, Mater. Lett. 278 (2020), 128417.
[2] EC2, Eurocode 2: Design of Concrete Structures. Part 1-1: General Rules and Rules for Buildings, CEN (European Committee for Standardization), 2010.
[3] ACI 318, Building Code Requeriments for Structural Concrete, 2019.
[4] K. Aghaee, K.H. Khayat, Effect of shrinkage-mitigating materials on performance of fiber-reinforced concrete – an overview, Construct. Build. Mater. 305 (2021), 124586.
[5] M.J. Abdolhosseini Qomi, L. Brochard, T. Honorio, I. Maruyama, M. Vandamme, Advances in atomistic modeling and understanding of drying shrinkage in cementitious materials, Cement Concr. Res. 148 (2021) V.
[6] N.P. Tran, C. Gunasekara, D.W. Law, S. Houshyar, S. Setunge, A. Cwirzen, A critical review on drying shrinkage mitigation strategies in cement-based materials, J. Build. Eng. 38 (2021), 102210.
[7] H. Zhang, J. Xiao, Plastic shrinkage and cracking of 3D printed mortar with recycled sand, Construct. Build. Mater. 302 (2021), 124405.
[8] F. Faleschini, P. Bragolusi, M.A. Zanini, P. Zampieri, C. Pellegrino, Experimental and numerical investigation on the cyclic behavior of RC beam column joints with EAF slag concrete, Eng. Struct. 152 (2017) 335–347.

[9] J.C. Salcedo, M. Fortea, The influence of structural alterations on the damages of the Amatrice earthquake, Italy, 2016, Inf. Constr. 72 (559) (2020) V.
[10] E. Tsolakis, C. Kalligeros, P. Tzouganakis, D. Koulocheris, V. Spitas, A novel experimental setup for the determination of the thermal expansion coefficient of concrete at cryogenic temperatures, Construct. Build. Mater. 309 (2021), 125134.
[11] R.V. Silva, J. De Brito, R.K. Dhir, Prediction of the shrinkage behavior of recycled aggregate concrete: a review, Construct. Build. Mater. 77 (2015) 327–339.
[12] ACI 209.2R, Guide for Modeling and Calculating Shrinkage and Creep in Hardened Concrete, 2008.
[13] C.Q. Lye, R.K. Dhir, G.S. Ghataora, Estimation models for creep and shrinkage of concrete made with natural, recycled and secondary aggregates, Mag. Concr. Res. 74 (8) (2022) 392–418.
[14] H.S. Müller, F. Acosta Urrea, V. Kvitsel, Creep and shrinkage prediction models for concrete, Beton- Stahlbetonbau 116 (9) (2021) 660–676.
[15] F. Xu, X. Lin, A. Zhou, Performance of internal curing materials in high-performance concrete: a review, Construct. Build. Mater. 311 (2021), 125250.
[16] S. Santos, P.R. da Silva, J. de Brito, Self-compacting concrete with recycled aggregates – a literature review, J. Build. Eng. 22 (2019) 349–371.
[17] J. Liu, N. Farzadnia, C. Shi, Microstructural and micromechanical characteristics of ultra-high performance concrete with superabsorbent polymer (SAP), Cement Concr. Res. 149 (2021), 106560.
[18] D. Wang, C. Shi, Z. Wu, J. Xiao, Z. Huang, Z. Fang, A review on ultra high performance concrete: Part II. Hydration, microstructure and properties, Construct. Build. Mater. 96 (2015) 368–377.
[19] J. Liu, C. Shi, X. Ma, K.H. Khayat, J. Zhang, D. Wang, An overview on the effect of internal curing on shrinkage of high performance cement-based materials, Construct. Build. Mater. 146 (2017) 702–712.
[20] L. Yang, C. Shi, Z. Wu, Mitigation techniques for autogenous shrinkage of ultra-high-performance concrete – a review, Compos. B Eng. 178 (2019), 107456.
[21] H. Okamura, Self-compacting high-performance concrete, Concr. Int. 19 (7) (1997) 50–54.
[22] J.M. Abdalhmid, A.F. Ashour, T. Sheehan, Long-term drying shrinkage of self-compacting concrete: experimental and analytical investigations, Construct. Build. Mater. 202 (2019) 825–837.
[23] F. Fiol, C. Thomas, J.M. Manso, I. López, Influence of recycled precast concrete aggregate on durability of concrete's physical processes, Appl. Sci. 10 (20) (2020) 7348.
[24] J. Duchesne, Alternative supplementary cementitious materials for sustainable concrete structures: a review on characterization and properties, Waste Biomass Valoris 12 (3) (2021) 1219–1236.
[25] M.G. Sohail, W. Alnahhal, A. Taha, K. Abdelaal, Sustainable alternative aggregates: characterization and influence on mechanical behavior of basalt fiber reinforced concrete, Construct. Build. Mater. 255 (2020), 119365.
[26] L. Świerczek, B.M. Cieślik, P. Konieczka, Challenges and opportunities related to the use of sewage sludge ash in cement-based building materials – a review, J. Clean. Prod. 287 (2021), 125054.
[27] D. Pedro, J. de Brito, L. Evangelista, Structural concrete with simultaneous incorporation of fine and coarse recycled concrete aggregates: mechanical, durability and long-term properties, Construct. Build. Mater. 154 (2017) 294–309.
[28] T. Ayub, W. Mahmood, A.U.R. Khan, Durability performance of scc and scgc containing recycled concrete aggregates: a comparative study, Sustainability 13 (15) (2021) 8621.
[29] J.J. Xu, W.G. Chen, C. Demartino, T.Y. Xie, Y. Yu, C.F. Fang, M. Xu, A Bayesian model updating approach applied to mechanical properties of recycled aggregate concrete under uniaxial or triaxial compression, Construct. Build. Mater. 301 (2021), 124274.
[30] Y. Tang, J. Xiao, H. Zhang, Z. Duan, B. Xia, Mechanical properties and uniaxial compressive stress-strain behavior of fully recycled aggregate concrete, Construct. Build. Mater. 323 (2022), 126546.
[31] J. Xiao, H. Zhang, J. de Brito, M.&S. highlight, Limbachiya, et al., Use of recycled aggregate in high-strength concrete, 2000, Mater. Struct. 55 (2) (2022) 40.
[32] R.V. Silva, J. de Brito, R.K. Dhir, Fresh-state performance of recycled aggregate concrete: a review, Construct. Build. Mater. 178 (2018) 19–31.
[33] A. Gonzalez-Corominas, M. Etxeberria, Effects of using recycled concrete aggregates on the shrinkage of high performance concrete, Construct. Build. Mater. 115 (2016) 32–41.
[34] V. Revilla-Cuesta, L. Evangelista, J. de Brito, V. Ortega-López, J.M. Manso, Effect of the maturity of recycled aggregates on the mechanical properties and autogenous and drying shrinkage of high-performance concrete, Construct. Build. Mater. 299 (2021), 124001.
[35] M.U. Hossain, J.C. Liu, D. Xuan, S.T. Ng, H. Ye, S.J. Abdulla, Designing sustainable concrete mixes with potentially alternative binder systems: multicriteria decision making process, J. Build. Eng. 45 (2022), 103587.
[36] M. Mahdikhani, M. Hatamiyan Sarvandani, Assessment of the bending bearing capacity of the GGBFS-based geopolymer concrete beams exposed to acidic environment, Arch. Civ. Mech. Eng. 21 (4) (2021) 160.
[37] H. Hafez, D. Kassim, R. Kurda, R.V. Silva, J. de Brito, Assessing the sustainability potential of alkali-activated concrete from electric arc furnace slag using the ECO2 framework, Construct. Build. Mater. 281 (2021), 122559.
[38] R.B. Tangadagi, M.M.D. Seth, P. S, Role of mineral admixtures on strength and durability of high strength self compacting concrete: an experimental study, Materials 18 (2021), 101144.
[39] M. Zajac, G. Bolte, J. Skocek, M. Ben Haha, Modelling the effect of the cement components fineness on performance and environmental impact of composite cements, Construct. Build. Mater. 276 (2021), 122108.
[40] C. Seneviratne, C. Gunasekara, D.W. Law, S. Setunge, D. Robert, Creep, shrinkage and permeation characteristics of geopolymer aggregate concrete: long-term performance, Arch. Civ. Mech. Eng. 20 (4) (2020) 140.
[41] J.R. Weng, W.C. Liao, Microstructure and shrinkage behavior of high-performance concrete containing supplementary cementitious materials, Construct. Build. Mater. 308 (2021), 125045.
[42] N. José, H. Ahmed, B. Miguel, E. Luís, B. Jorge, Magnesia (MgO) production and characterization, and its influence on the performance of cementitious materials: a review, Materials 13 (21) (2020) 4752.
[43] R. Rodríguez-Álvaro, B. González-Fonteboa, S. Seara-Paz, K.M.A. Hossain, Internally cured high performance concrete with magnesium based expansive agent using coal bottom ash particles as water reservoirs, Construct. Build. Mater. 251 (2020), 118977.
[44] J.A. Forero, M. Bravo, J. Pacheco, J. de Brito, L. Evangelista, Fracture behaviour of concrete with reactive magnesium oxide as alternative binder, Appl. Sci. 11 (7) (2021) 2891.
[45] T. Gonçalves, R.V. Silva, J. de Brito, J.M. Fernández, A.R. Esquinas, Mechanical and durability performance of mortars with fine recycled concrete aggregates and reactive magnesium oxide as partial cement replacement, Cement Concr. Compos. 105 (2020), 103420.
[46] V. Revilla-Cuesta, L. Evangelista, J. de Brito, M. Skaf, V. Ortega-López, Mechanical performance and autogenous and drying shrinkage of MgO-based recycled aggregate high-performance concrete, Construct. Build. Mater. 314 (2022), 125726.
[47] Y. Mao, J. Liu, C. Shi, Autogenous shrinkage and drying shrinkage of recycled aggregate concrete: a review, J. Clean. Prod. 295 (2021), 126435.
[48] Q. Wang, Y. Geng, Y. Wang, H. Zhang, Drying shrinkage model for recycled aggregate concrete accounting for the influence of parent concrete, Eng. Struct. 202 (2020), 109888.
[49] H. Zhang, Y.Y. Wang, D.E. Lehman, Y. Geng, Autogenous-shrinkage model for concrete with coarse and fine recycled aggregate, Cement Concr. Compos. 111 (2020), 103600.
[50] EN-Euronorm, Rue de stassart, 36. Belgium-1050 Brussels, European Committee for Standardization.
[51] A. Santamaría, J.J. González, M.M. Losáñez, M. Skaf, V. Ortega-López, The design of self-compacting structural mortar containing steelmaking slags as aggregate, Cement Concr. Compos. 111 (2020), 103627.
[52] S. Park, S. Wu, Z. Liu, S. Pyo, The role of supplementary cementitious materials (Scms) in ultra high performance concrete (uhpc): a review, Materials 14 (6) (2021) 1472.
[53] A. Santamaría, V. Ortega-López, M. Skaf, J.A. Chica, J.M. Manso, The study of properties and behavior of self compacting concrete containing Electric Arc Furnace Slag (EAFS) as aggregate, Ain Shams Eng. J. 11 (1) (2020) 231–243.
[54] F. Agrela, M. Sánchez De Juan, J. Ayuso, V.L. Geraldes, J.R. Jiménez, Limiting properties in the characterisation of mixed recycled aggregates for use in the manufacture of concrete, Construct. Build. Mater. 25 (10) (2011) 3950–3955.
[55] V. Revilla-Cuesta, V. Ortega-López, M. Skaf, J.M. Manso, Effect of fine recycled concrete aggregate on the mechanical behavior of self-compacting concrete, Construct. Build. Mater. 263 (2020), 120671.
[56] A.S. Brand, J.R. Roesler, A. Salas, Initial moisture and mixing effects on higher quality recycled coarse aggregate concrete, Construct. Build. Mater. 79 (2015) 83–89.
[57] LNEC-E398, Determination of Drying Shrinkage and Expansion (In Portuguese), National Laboratory in Civil Engineering (LNEC – Laboratório Nacional de Engenharia Civil), Lisbon, Portugal, 1993.
[58] R. Lanti, M. Martínez, Biaxial bending and axial load in reinforced concrete sections, Numer. Aproach Inf. Constr. 72 (558) (2020) 1–9.
[59] M. Bravo, J. De Brito, J. Pontes, L. Evangelista, Shrinkage and creep performance of concrete with recycled aggregates from CDW plants, Mag. Concr. Res. 69 (19) (2017) 974–995.
[60] M. Bravo, J. De Brito, J. Pontes, L. Evangelista, Mechanical performance of concrete made with aggregates from construction and demolition waste recycling plants, J. Clean. Prod. 99 (2015) 59–74.
[61] H.M. Tran, A. Scott, Strength and workability of magnesium silicate hydrate binder systems, Construct. Build. Mater. 131 (2017) 526–535.
[62] V. Revilla-Cuesta, M. Skaf, A. Santamaría, J.J. Hernández-Bagaces, V. Ortega-López, Temporal flowability evolution of slag-based self-compacting concrete with recycled concrete aggregate, J. Clean. Prod. 299 (2021), 126890.
[63] A. Gonzalez-Corominas, M. Etxeberria, C.S. Poon, Influence of steam curing on the pore structures and mechanical properties of fly-ash high performance concrete prepared with recycled aggregates, Cement Concr. Compos. 71 (2016) 77–84.
[64] S.C. Kou, C.S. Poon, Effect of the quality of parent concrete on the properties of high performance recycled aggregate concrete, Construct. Build. Mater. 77 (2015) 501–508.
[65] A. Sahraei Moghadam, F. Omidinasab, M. Abdalikia, The effect of initial strength of concrete wastes on the fresh and hardened properties of recycled concrete reinforced with recycled steel fibers, Construct. Build. Mater. 300 (2021), 124284.
[66] A. Sahraei Moghadam, F. Omidinasab, S. Moazami Goodarzi, Characterization of concrete containing RCA and GGBFS: mechanical, microstructural and environmental properties, Construct. Build. Mater. 289 (2021), 123134.
[67] M. Jalal, N. Nassir, H. Jalal, Waste tire rubber and pozzolans in concrete: a trade-off between cleaner production and mechanical properties in a greener concrete, J. Clean. Prod. 238 (2019), 117882.

[68] M. Behera, A.K. Minocha, S.K. Bhattacharyya, Flow behavior, microstructure, strength and shrinkage properties of self-compacting concrete incorporating recycled fine aggregate, Construct. Build. Mater. 228 (2019), 116819.
[69] S. Altoubat, D. Badran, M.T. Junaid, M. Leblouba, Restrained shrinkage behavior of Self-Compacting Concrete containing ground-granulated blast-furnace slag, Construct. Build. Mater. 129 (2016) 98–105.
[70] M. Velay-Lizancos, J.L. Perez-Ordoñez, I. Martinez-Lage, P. Vazquez-Burgo, Analytical and genetic programming model of compressive strength of eco concretes by NDT according to curing temperature, Construct. Build. Mater. 144 (2017) 195–206.